

Analyst

Accepted Manuscript



This is an *Accepted Manuscript*, which has been through the Royal Society of Chemistry peer review process and has been accepted for publication.

Accepted Manuscripts are published online shortly after acceptance, before technical editing, formatting and proof reading. Using this free service, authors can make their results available to the community, in citable form, before we publish the edited article. We will replace this *Accepted Manuscript* with the edited and formatted *Advance Article* as soon as it is available.

You can find more information about *Accepted Manuscripts* in the [Information for Authors](#).

Please note that technical editing may introduce minor changes to the text and/or graphics, which may alter content. The journal's standard [Terms & Conditions](#) and the [Ethical guidelines](#) still apply. In no event shall the Royal Society of Chemistry be held responsible for any errors or omissions in this *Accepted Manuscript* or any consequences arising from the use of any information it contains.

1
2
3 Resolving Powers of >7900 Using Linked Scans: How Well Does Resolving Power
4 Describe the Separation Capability of Differential Ion Mobility Spectrometry
5
6

7 Brandon G. Santiago, Rachel A. Harris, Samantha L. Isenberg, Gary L. Glish
8
9

10
11 Department of Chemistry, Caudill and Kenan Laboratories, The University of North
12 Carolina at Chapel Hill, Chapel Hill, NC 27599-3290, USA
13
14
15
16
17
18
19
20
21
22
23
24
25
26
27
28
29
30
31
32
33
34
35
36
37
38
39
40
41

42 Address reprint requests to:

43 Gary L. Glish

44 Department of Chemistry
45

46 Campus Box 3290
47
48

49 Caudill Laboratories
50

51 The University of North Carolina at Chapel Hill

52 Chapel Hill NC, 27599-3290

53 919-962-2303

54 919-962-2388 (fax)

55 glish@unc.edu
56
57
58
59
60

Abstract

Differential ion mobility spectrometry (DIMS) separations are described using similar terminology to liquid chromatography, capillary electrophoresis, and drift tube ion mobility spectrometry. The characterization and comparison of all these separations are typically explained in terms of resolving power, resolution, and/or peak capacity. A major difference between these separations is that DIMS separations are in space whereas the others are separations in time. However, whereas separations in time can, in theory, be extended infinitely, separations in space, such as DIMS separations, are constrained by the physical dimensions of the device. One method to increase resolving power of DIMS separations is to use helium in the DIMS carrier gas. However, ions have a greater mobility in helium which causes more ions to be neutralized due to collisions with the DIMS electrodes or electrode housing, i.e. the space constraints. This neutralization of ions can lead to the loss of an entire peak, or peaks, from a DIMS scan. To take advantage of the benefits of helium use while reducing ion losses, linked scans were developed. During a linked scan the amount of helium present in the DIMS carrier gas is decreased as the compensation field is increased. A comparison of linked scans to compensation field scans with constant helium is presented herein. Resolving powers >7900 are obtained with linked scans. However, this result highlights the limitation of using resolving power as a metric to describe DIMS separations.

Introduction

Post-ionization separation techniques have been used increasingly in the field of mass spectrometry when analyzing complex mixtures. These gas phase separations, such as ion mobility spectrometry (IMS), can be used as a discrete separation step or in conjunction with pre-ionization condensed phase separations. The most employed ion mobility techniques, drift tube ion mobility spectrometry (DT-IMS) and travelling wave ion mobility spectrometry (TWIMS), separate ions based on their absolute mobility (K_l , $\text{cm}^2 \text{V}^{-1} \text{sec}^{-1}$) in low electric fields.^{1, 2} In the electric field regimes used in these techniques an ion's mobility is independent of field strength and can be described by the Mason-Schamp equation.³ However, when the electric field strength exceeds some value (typically estimated to be around 10,000 V/cm), this direct relationship is no longer valid and ion mobility changes based on field strength in a complex function.²⁻⁶

Differential ion mobility spectrometry (DIMS) uses this difference in mobilities in high versus low electric fields to separate ions in space, rather than in time. A DIMS device consists of two parallel electrodes separated by a gap, typically on the order of 0.30 to 2.0 mm in height.⁷⁻¹² Contrary to DT-IMS, where a voltage gradient draws ions through the drift tube and ions are separated in time, the gas flow through the DIMS electrodes accounts for the ion motion from the entrance of the DIMS device to the exit, while the mobility separation occurs orthogonal to the gas flow. An asymmetric rf waveform is applied across the electrode gap, the V_{0-P} which is referred to as the dispersion field (E_D) when divided by the gap size. This

1
2
3 waveform alternates between low and high electric fields of opposing polarity
4
5 causing the ions to oscillate in the direction of the electrodes.
6
7

8
9 Due to the alternating polarities and the design of the waveform, the net
10 displacement is zero if the high field mobility (K_h) and low field mobility (K_l) are
11 equal. However, if $K_h \neq K_l$ a net displacement is obtained during one period of the
12 waveform, which is integrated across the number of periods the waveform will
13 undergo during the ion's transit through DIMS. If this net displacement becomes too
14 large at any point during transit through DIMS the ion will collide with an electrode
15 and be neutralized. Alternatively, the displacement can be offset by the use of a dc
16 compensation field to counterbalance the difference between K_h and K_l , allowing
17 ions with a selected difference in mobilities to pass through the DIMS device. The
18 applied compensation field can be held constant, causing DIMS to act as a filter for a
19 selected analyte ion, or scanned to sequentially pass ions of various differential ion
20 mobilities.^{3, 13}
21
22
23
24
25
26
27
28
29
30
31
32
33
34
35
36

37 DIMS separation characteristics are commonly reported in a similar manner
38 to chromatographic methods and DT-IMS. As such resolving power, resolution, and
39 peak capacity are often used to describe the separations.^{7, 10, 11, 14-16} Resolving power
40 is the most commonly reported value for DIMS separations due to its ease of use.
41
42 The resolving power of a DIMS separation can be calculated using Equation 1, and
43 depends only on the compensation field required to pass an analyte through DIMS
44 and the width of that peak, measured as a full width at half maximum.¹⁰ Therefore,
45 calculating the resolving power of a DIMS separation requires only one analyte be
46 used, and has previously been described as an adequate way to compare separation
47
48
49
50
51
52
53
54
55
56
57
58
59
60

abilities across DIMS devices.¹⁶ Alternatively, the resolution between two peaks requiring different compensation fields (E_{C1} and E_{C2}) can be calculated (Equation 2), or the peak capacity of the entire separation can be determined.¹⁰ These values are preferred over resolving power because they describe the separation that is occurring, rather than expressing the theoretical separation capabilities of a DIMS device.¹⁷

$$\text{Resolving Power} = \frac{E_C}{(FWHM)} \quad (1)$$

$$\text{Resolution} = \frac{E_{C1} - E_{C2}}{\left(\frac{w_1 + w_2}{2}\right)} = \frac{1.178 (E_{C1} - E_{C2})}{(FWHM_1 + FWHM_2)} \quad (2)$$

One method to improve DIMS separations is to vary the composition of the DIMS carrier gas by mixing gases such as helium, oxygen, or carbon dioxide into the typically nitrogen carrier gas or replacing the nitrogen completely.^{7, 16, 18-20} The mostly commonly used alternative gas is helium, which increases the differential ion mobility for all ions, although not equally. Ions with a higher differential ion mobility in nitrogen tend to require higher absolute increases in compensation field upon the addition of helium to the carrier gas. Although this is not universal, the general result is increased dispersion in the compensation field domain and improvement of DIMS separations.^{8, 17}

However, the use of helium also results in a decrease in signal intensity resulting from the collisions of ions with either the DIMS electrodes or the housing containing the electrodes. This increase in ion collisions with the electrodes and housing stems from the differences in ion mobility through the smaller, less polarizable helium.¹⁸ In comparison to nitrogen, helium decreases the reduced

1
2
3 mass, the collisional cross-section, and long-range interactions of the collision
4
5 partners.^{10, 21} These changes produce a greater difference between K_l and K_h and
6
7 cause greater displacement during each period of the waveform, increasing the
8
9 likelihood that ions will strike an electrode and be neutralized. Additionally, the ion
10
11 motion parallel to the electrodes and transverse to the carrier gas flow is dictated by
12
13 K_l at all times. The addition of helium to the carrier gas increases K_l making the ions
14
15 more likely to diffuse the width of the electrodes and be neutralized on the housing.
16
17 ²¹ One can think of this from the perspective of the space of the separation. With the
18
19 addition of helium and increased ion mobilities, the ions spread out into a greater
20
21 space, but the available space is fixed by the dimensions of the device. This is very
22
23 different from chromatographic and DT-IMS separations, where lengthening the
24
25 separation time increases band broadening due to diffusion, yet the peaks are still
26
27 detected. The physical dimensions of the electrode gap in DIMS set a limit upon the
28
29 maximum allowable amount of diffusion. Beyond that the ions are neutralized upon
30
31 collision with the DIMS housing and not detected.
32
33
34
35
36
37
38

39 To combine the benefits of using helium, while reducing the loss of ions,
40
41 linked scans of the carrier gas composition and the compensation field were
42
43 developed.¹⁷ As the compensation field is increased, the amount of helium present
44
45 in the carrier gas is reduced. An example scan is shown in Figure 1, where the
46
47 amount of helium in the carrier gas is lowered from 40% to 0% as the compensation
48
49 field is scanned. This technique has been shown to improve the separation
50
51 capabilities of DIMS, specifically the resolution between analytes and peak capacity
52
53 of a DIMS separation, while also reducing ion losses to neutralization.¹⁷ The work
54
55
56
57
58
59
60

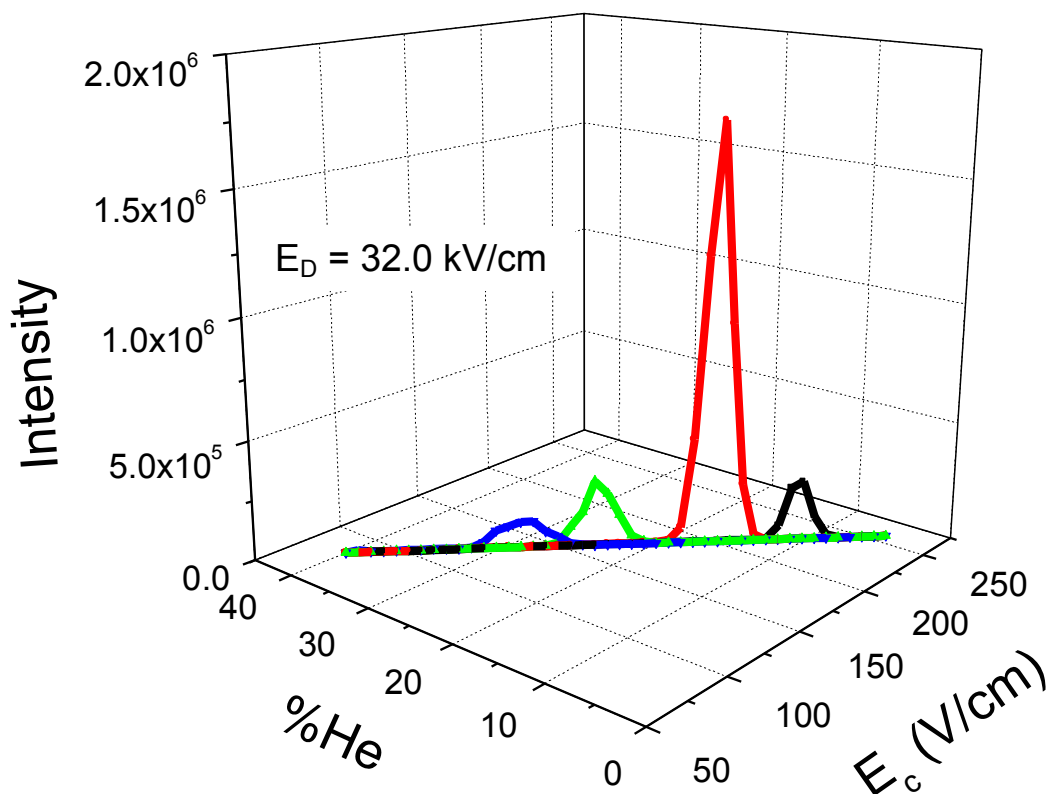


Figure 1. A representative linked scan during which m/z 622 (black), 922 (red), 1522 (green), and 2122 (blue, intensity $\times 5$) from Agilent ESI tuning mix are separated. Here the helium is decreased from 40% to 0% as the compensation field is scanned

presented herein describes the influence that the rate at which helium is reduced with respect to compensation field has on the resolving power and resolution of DIMS separations.

Results and Discussion

The use of resolving power as a metric to describe DIMS separations has become commonplace because it allows for the rapid characterization and comparison of DIMS separations. To begin to compare linked scans and compensation field scans with constant helium, the resolving power of peaks from three charge states of the protein ubiquitin were examined. For this work, the

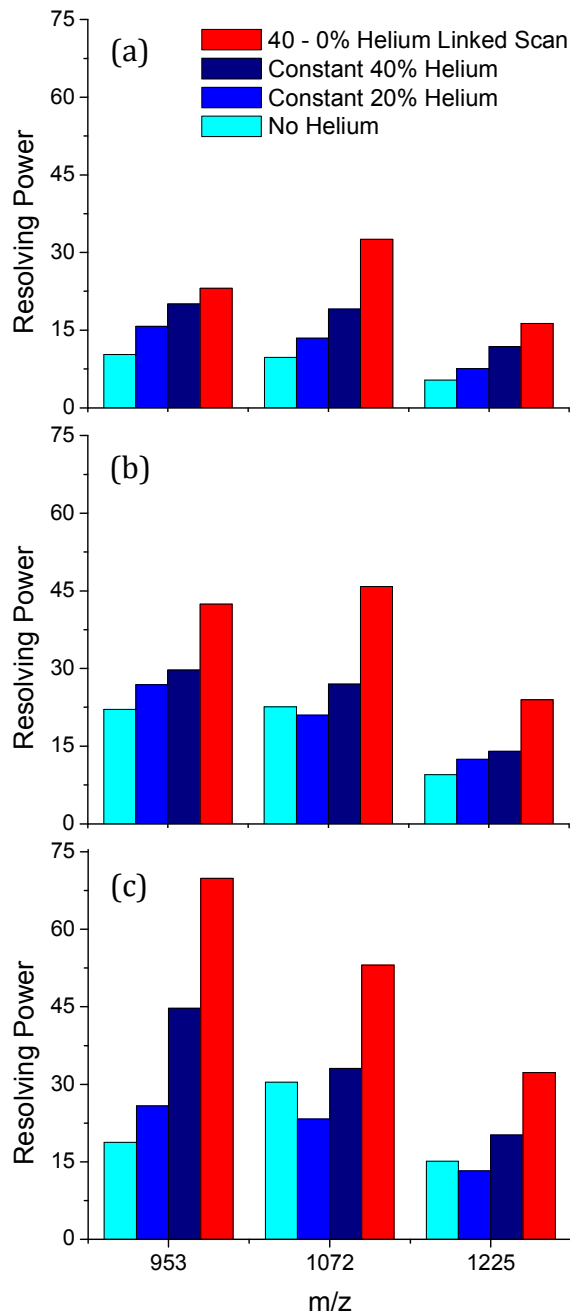


Figure 2. Plots comparing the resolving powers for three charge states of ubiquitin. Compensation field scans with constant helium and linked scans from 40 - 0% helium are shown at E_D of (a) 26.0 kV/cm, (b) 30.0 kV/cm, and (c) 34.0 kV/cm. The 9+ charge state of ubiquitin presented multiple peaks during DIMS scans. Peak statistics were taken for the most abundant peak, which required the highest compensation field to pass through DIMS

helium content of the carrier gas was lowered linearly from 40 to 0% during linked scans as the compensation field was linearly increased. These linked scans were compared to compensation field scans with 0, 20, or 40% constant helium. Shown in Figure 2, it was observed that for the 7+ (m/z 1225), 8+ (m/z 1072), and 9+ (m/z 953) charge states of ubiquitin linked scans yield higher resolving powers. At dispersion fields of 26.0, 30.0, and 34.0 kV/cm linked scans improved resolving power by an average of 54% over compensation field scans with 40% constant helium. Even greater gains in resolving power are observed for the 40 - 0% linked scans when compared to compensation field scans with 0

1
2
3 and 20% constant helium, as the compensation field scans with lower amounts of
4
5 helium yielded lower resolving powers.
6
7

8 The previous use of linked scans gave improved resolving powers, even
9
10 though the ions passed through DIMS at lower than 40% helium during linked
11
12 scans. For example, the linked scan in Figure 1 begins with 40% helium yet the
13
14 peaks for m/z 1522 and 922 pass through DIMS at 23.8 and 16.1% helium,
15
16 respectively. A lower amount of helium leads to lower differential ion mobility,
17
18 yielding lower resolving powers. Thus it was believed that to more accurately
19
20 portray the improvements of linked scans, peaks should be compared to
21
22 compensation field scans with constant helium at the same helium percentage
23
24 present at the centroid of each peak in the linked scan. For this assessment the
25
26 resolving powers of four peaks from Agilent ESI tuning mix were compared for
27
28 linked scans and compensation field scans with constant helium. Compensation field
29
30 scans with constant helium were taken in 5% increments from 0 to 60% at a
31
32 dispersion field of 28.0 kV/cm, and the resolving power of the linked scan peak was
33
34 compared to the compensation field scan with the closest amount of constant
35
36 helium. To clarify, one experiment gave the peak for m/z 922 to be centered at
37
38 16.1% helium in the helium domain during a linked scan. The resolving power of
39
40 this peak was compared to a compensation field scan with constant 15% helium
41
42 present in the carrier gas. The results presented in Figure 3 show that linked scans
43
44 from 20-0, 40-0, and 60-0% helium improve the resolving powers of the four
45
46 analyte ions (m/z 622, 922, 1522, and 2122) versus compensation field scans with
47
48 constant helium.
49
50
51
52
53
54
55
56
57
58
59
60

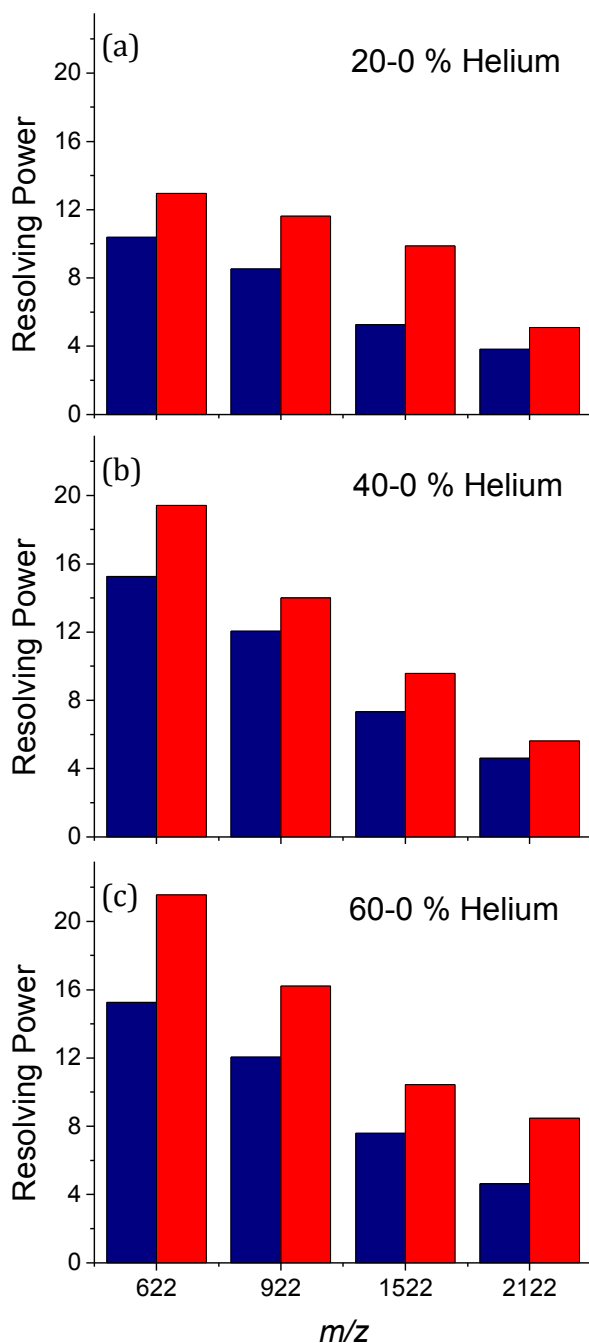


Figure 3. Plots comparing the resolving power of linked scans (red) to compensation field scans with constant helium (blue). The scans with constant helium were taken with approximately the same helium content that was present when the peaks passed through DIMS in the linked scan. The linked scan helium ranges shown are (a) 20-0%, (b) 40-0%, and (c) 60-0% helium

Despite these promising results it was suspected that the point in the helium/compensation field scans at which the peak passed through DIMS might be causing inconsistencies in the data. For example, a higher amount of helium in the carrier gas causes higher required compensation fields for the ubiquitin peaks. However, if the scanned compensation field range was not properly adjusted when increasing the helium range of a linked scan, the peaks would pass through DIMS after more steps were taken in the compensation

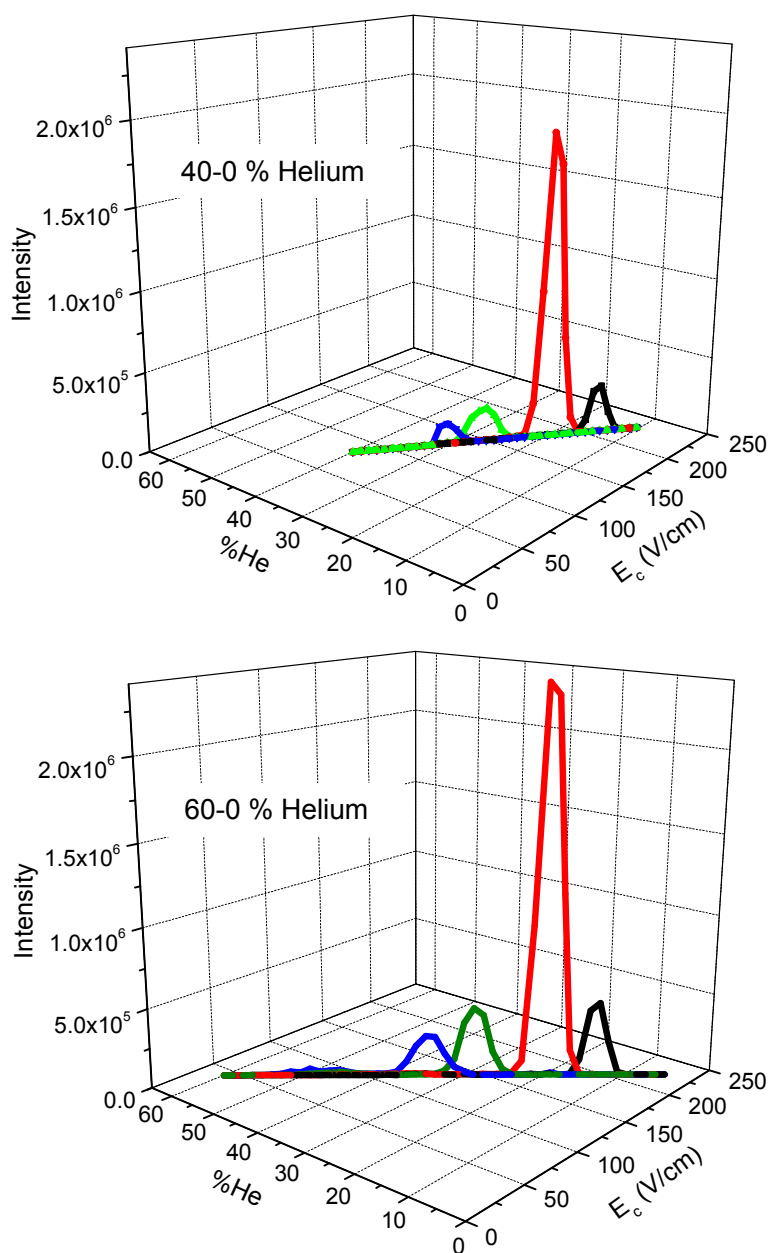


Figure 4. Plots showing how the scanned compensation field range was changed between (a) 40-0% and (b) 60-0% helium linked scans

field and helium domains.

This can be seen in Figure

4 where rather than

shifting the entire

compensation field range

as the helium scan range

moved from 40-0 to 60-

0%, the compensation

field range was extended

on the lower end. Based

on the relationship

between ion mobility and

helium, this causes the

peaks to pass through

DIMS after significantly

more compensation field

steps. Thus, the ions

would pass through DIMS

at a lower helium content

and have lower than

expected differential ion mobilities, necessitating lower compensation fields to

correct for their net displacement. In Figure 4, this essentially results in the peaks in

the two scans passing through DIMS at the same required compensation fields,

rather than a higher helium range raising the required compensation fields. A similar effect could be expected when increasing dispersion field, which also increases the required compensation fields for the ubiquitin peaks.

Based on these studies it was determined that the peak position in both the helium domain and compensation field domain needed to be controlled to allow for the true value of linked scans to be determined. Therefore, compensation field scans were performed with the peak centroid of m/z 922 held constant in both domains. This allowed for the effect of passing through this point at an angle, such as in a linked scan, to be compared to a compensation field scan with constant helium. Holding the centroid constant in the two dimensions while changing the rate at which the helium content is lowered with respect to compensation field is depicted in Figure 5. Here it can be observed how changing the slope of the linked scan affects the intersection of the linked scan line and the stable trajectories through

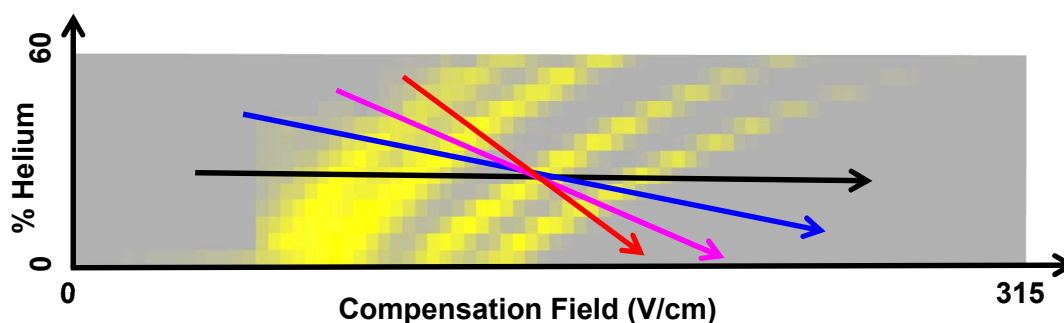


Figure 5. Normalized intensities for m/z 2122, 1522, 922 and 622 (left to right) as a function of helium and compensation field. The intensity (shown in yellow) depicts stable trajectories through the DIMS device. The black (constant helium), blue, magenta, and red arrows, respectively, are indicative of increasing the rate at which helium is changed with regards to compensation field. The common intersection of the arrows is representative of keeping the peak centroid for m/z 922 constant in the helium and compensation field domains

DIMS. The effect of this slope on resolving power is shown in Figure 6. At dispersion fields of 24.0 and 32.0 kV/cm it is observed that changing the slope of the helium scan with respect to compensation field increases the resolving power for m/z 922 in a linear fashion.

In an attempt to maximize resolving power, the slope of the helium scan was further increased, the results of which can be seen in Figure 7a. Increasing the helium scan rate to (90% Helium)/(V/cm) increases the resolving powers for m/z 922 and m/z 1522 to 1573 and 1716, respectively, at 31.0 kV/cm. These values are over 3 times greater than the best reported value in the literature of 500.²² However, during these experiments it was observed that as the resolving power increased for the two peaks, the ability to separate the two analytes stayed constant. Upon calculation of the resolution between the two peaks, it was observed that

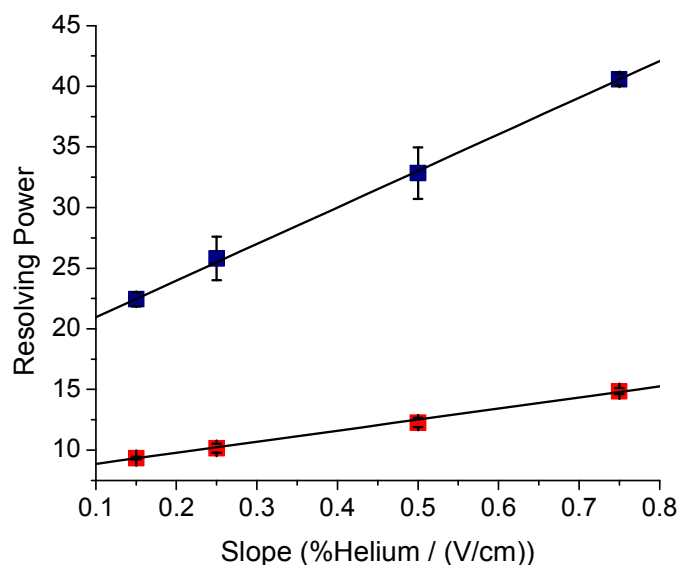


Figure 6. Plots of resolving power versus the rate at which helium percentage is lowered with respect to compensation field at dispersion fields of 24.0 kV/cm (red) and 32.0 kV/cm (blue)

despite the impressive gains in resolving power no improvement in resolution was measured (Figure 7b). This seemingly contradictory result stems from the manner in which resolving power is calculated. Resolving power is determined solely based on the required compensation

1
2
3 field and the width of the
4
5 peak, measured as the full
6
7 width at half maximum in
8
9 the compensation field
10
11 domain. By changing the
12
13 slope of the helium scan the
14
15 peak width is narrowed is
16
17

18
19 regards to the
20
21 compensation field domain.
22

23
24 The peak FWHM were
25
26 reduced from an average of
27
28 21.8 V/cm with no helium
29
30 present to 0.1 V/cm at the
31
32 highest slope. However, at
33
34

35
36 the same time the distance
37
38 between the peak centroids
39
40 was decreased from 36.8 to
41
42 0.3 V/cm. The combination
43
44 of these factors yields
45
46

47
48
49 impressive resolving powers but no improvement in resolution between the two
50
51 peaks. As such, resolving power is inadequate to describe the separation capabilities
52
53 of linked scans.
54
55
56
57
58
59
60

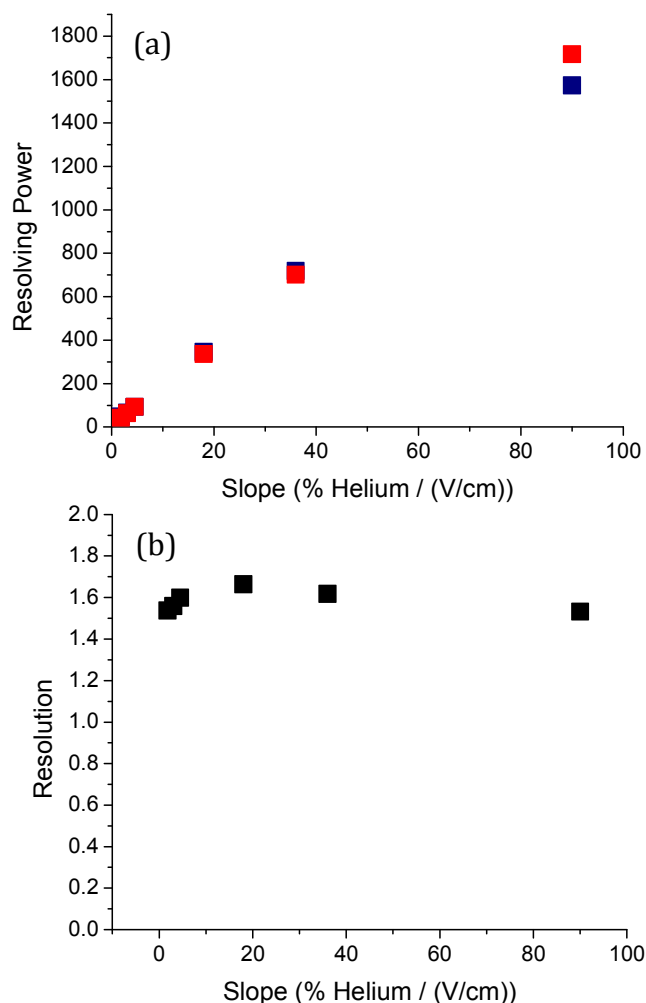


Figure 7. (a) Plot showing the effect on resolving power of increasing the rate at which helium content is lowered relative to compensation field. The resolving powers for m/z 922 (blue) and m/z 1522 (red) reach 1573 and 1716, respectively. (b) Plot of resolution versus the rate at which helium content is lowered relative to compensation field

To further compare the resolving powers attained using linked scans to those reported in the literature, the effect of slope was investigated using the peptide syntide 2.^{8, 15, 16, 22, 23} Multiple peaks were observed for the triply charged species during compensation field scans, however, only the most intense DIMS peak was analyzed in a similar manner as the peak for m/z 922 in the previous experiment. Holding the peak centroid constant in both the compensation field and helium domains, increasing the slope of the helium scan with respect to the compensation field scan once again increased resolving power in a linear fashion (Figure 8). At a dispersion field of 28.7 kV/cm, resolving powers above 7900 were obtained using syntide 2. This value is consistent with the values obtained for m/z 922 from Agilent ESI tuning mix as the syntide peak was more narrow (12.4 V/cm versus 19.3 V/cm) during compensation field scans with no helium present, and the compensation field centroid used during this slope experiment for syntide 2 (3+) was higher (327.9 V/cm versus 170.5 V/cm). The resultant resolving power is over 16 times greater than the best previously reported value,

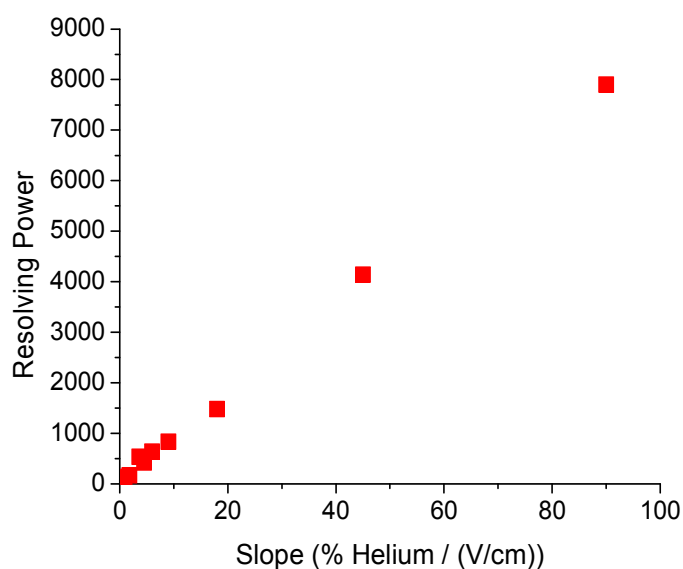


Figure 8. Plot showing the effect on resolving power of increasing the rate at which helium content is lowered relative to compensation field. The resolving powers for syntide 2 (3+) reaches 7903 (FWHM = 0.04 V/cm) at the highest slope used

1
2
3 however, as stated above the increase in resolving power does not correlate to
4
5 improvement in the separation capabilities of the device.²²
6
7

8
9 It should be noted that the resolving power of a peak is dependent on a
10 number of attributes of the device. Parameters such as the ion transit time through
11 DIMS and the reduced electric field strength used affect the resolving power
12 measured.²³ For example, at a dispersion field of 28.7 kV/cm and constant 40%
13 helium carrier gas the DIMS device discussed in this work gave a resolving power of
14 30.1 for syntide 2 (3+). Under those conditions the DIMS device that produced
15 resolving powers of 500 yielded a resolving power of 175 for syntide 2 (3+).¹⁶ Thus
16
17 it could be expected that the combination of the linked scans discussed here and the
18 DIMS device described elsewhere would yield even greater resolving powers.
19
20
21
22
23
24
25
26
27
28
29

30 Additionally, because DIMS separates ions based on their differences in
31 mobilities between the high and low fields, a higher resolving power stemming from
32 a greater required compensation field gives little information about ion motion
33 within the DIMS gap. In chromatographic and DT-IMS separations it can be expected
34 that all peaks will be detected, the last of which will have the highest resolving
35 power. In DIMS, the spatial restrictions set by the physical dimensions disallow
36 these generalizations. Ion populations with a greater differential ion mobility than
37 that of the ion used to report resolving power can be entirely lost due to collisions
38 with the electrodes. Alternatively, ion populations with large K_l and K_h can require
39 minimal compensation field, yet be lost by diffusion to the DIMS housing or to an
40 electrode due to an oscillation during one portion of the waveform. Thus, in either
41 case the number of analyte peaks detected is lowered, even though the reported
42
43
44
45
46
47
48
49
50
51
52
53
54
55
56
57
58
59
60

1
2
3 resolving power is increased. This decrease in peak capacity upon the addition of
4
5 greater percentages of constant helium has been previously shown, whereas linked
6
7 scans were shown to improve the resolution between peaks and increase peak
8
9 capacity at greater helium percentages, all while also reducing the amount of ion
10
11 loss due to neutralization.¹⁷
12
13

14 **Experimental**

15
16 Methanol (optima grade), acetonitrile (optima grade), water (HPLC grade),
17
18 and acetic acid (ACS plus) were purchased from Fisher Scientific (Fairlawn, NJ, USA).
19
20 Ubiquitin from bovine red blood cells (min. 90% by SDS Page) and syntide 2 (min.
21
22 95% by HPLC) were purchased from Sigma (St. Louis, MO, USA). Ubiquitin was
23
24 diluted to 5 μM in 50/49/1 methanol/water/acetic acid. Syntide 2 was diluted to 6.7
25
26 μM in 50/49/1 methanol/water/acetic acid. Agilent ESI tuning mix was diluted 20
27
28 fold in 95/5 acetonitrile/water. Samples were infused for electrospray ionization
29
30 (ESI) at 2 $\mu\text{L}/\text{min}$. Experiments were performed on a Bruker Esquire 3000 ion trap
31
32 mass spectrometer. Ubiquitin and Agilent ESI tuning mix experiments were
33
34 conducted with +4.25 kV applied to the electrospray emitter. Syntide 2 experiments
35
36 were performed with +3.0 kV applied to the electrospray emitter, as the lower
37
38 voltage yielded greater signal intensity. The instrument software was used to set the
39
40 ESI desolvation gas flow rate to 1.0 L/min and temperature to 300° C. This gas flow
41
42 was combined with a supplemental gas flow provided by two mass flow controllers
43
44 such that the total desolvation gas flow was maintained at 5.0 L/min (discussed
45
46 below).
47
48
49
50
51
52
53
54
55
56
57
58
59
60

1
2
3
4
5
6
7
8
9
10
11
12
13
14
15
16
17
18
19
20
21
22
23
24
25
26
27
28
29
30
31
32
33
34
35
36
37
38
39
40
41
42
43
44
45
46
47
48
49
50
51
52
53
54
55
56
57
58
59
60

A previously described planar DIMS assembly threads onto the Apollo I source of the Bruker Esquire 3000 ion trap mass spectrometer, replacing the spray shield.^{7,17} An O-ring seal joins the assembly to the custom flared glass transfer capillary, allowing the gas flow into the mass spectrometer to draw ions through the gap between the electrodes.²⁴ The DIMS assembly is designed such that the nitrogen desolvation gas used in the Apollo I source is rerouted through the DIMS assembly and performs the roles of both desolvation gas and DIMS carrier gas.

DIMS scans were controlled using a LabVIEW program interfaced to the instrument control software. The compensation voltage was increased after every 10 mass spectra recorded by the instrument. The LabVIEW output was also used to control the presence of helium in the carrier gas. The LabVIEW output directly controlled a MKS model 1179 nitrogen mass flow controller, whereas this output and a difference amplifier controlled an Alicat MC-10SLPM-D helium mass flow controller. In this way, the flow out of the mass flow controllers always summed to 4.0 L/min and could be added to the 1.0 L/min desolvation gas flow from the Bruker Esquire 3000. Linked scans were performed by scanning the output voltage from LabVIEW, thus lowering the amount of helium present in the carrier gas as the compensation field was increased. These linked scans were compared to compensation field scans with constant amounts of helium present in the carrier gas.

The dispersion voltage and compensation voltage were supplied by a custom-built power supply. The power supply outputs two sinusoidal waveforms approximately 90° phase shifted that are 1.7 and 3.4 MHz in frequency and 2:1 in

1
2
3 amplitude, respectively. Each of these waveforms is applied to a DIMS electrode, and
4
5 the capacitive coupling across the DIMS gap creates a bisinusoidal waveform with a
6
7 form parameter of 0.67.²⁵ For the experiments herein, dispersion fields ranged from
8
9 24.0 to 32.0 kV/cm and compensation fields ranged from 0 to 400 V/cm.
10
11

12
13 Both linked scans and compensation field scans with constant helium can be
14
15 displayed by plotting either the total ion current or the extracted ion current as a
16
17 function of the applied compensation field. Peak centroids and full width at half
18
19 maximum were calculated using either a Wolfram Mathematica 7.0 script or
20
21 Microcal Origin 6.0, both under the assumption of Gaussian distributions. The
22
23 program utilized for peak characterization was consistent within each comparison.
24
25 These values were used in conjunction with Equations 1 and 2 to calculate resolving
26
27 powers and/or resolution between peaks, respectively.
28
29
30
31

32 **Conclusion**

33
34 Varying the rate at which the helium percentage in the carrier gas was
35
36 changed with respect to compensation field yielded a linear increase in the
37
38 measured resolving power. This method was used to obtain resolving powers of
39
40 over 7900; more than 16 times greater than the previously best reported value.
41
42 However, while these linked scans provide significant increases in resolving power
43
44 over compensation field scans with constant helium, these increases in resolving
45
46 power do not translate to increases in resolution between peaks. For these
47
48 particular analytes the resolution between them was relatively constant. Thus,
49
50 resolving power was unable to accurately describe the separations taking place
51
52 during linked scans. The physical restrictions set by the dimensions of the DIMS gap,
53
54
55
56
57
58
59
60

1
2
3 in combination with DIMS separations being based on differential ion mobility,
4
5 makes resolving power an uninformative value for describing the separation
6
7 capabilities of a DIMS device. Instead, metrics such as resolution and or peak
8
9 capacity should be used. Using these metrics linked scans do provide improved
10
11 performance over conventional compensation field scans in DIMS, although not
12
13 nearly as drastically as the resolving power increase would suggest.
14
15
16

17 **Acknowledgements**

18 Support for this work was provided by R. J. Reynolds Tobacco Co.
19
20
21
22
23
24
25

26 **References**

- 27
28 1 A. A. Shvartsburg and R. D. Smith, *Anal. Chem.*, 2008, **80**, 9689-9699.
29
30 2 G. A. Eiceman and Z. Karpas, *Ion Mobility Spectrometry*, CRC Press, 2005.
31
32 3 A. A. Shvartsburg, *Differential ion mobility spectrometry : nonlinear ion transport*
33 *and fundamentals of FAIMS*, CRC Press, Boca Raton, 2009.
34
35 4 E. A. Mason and E. W. McDaniel, *Transport Properties of Ions in Gases*, Wiley, New
36 York, 1988.
37
38 5 R. W. Purves, R. Guevremont, S. Day, C. W. Pipich and M. S. Matyjaszczyk, *Rev. Sci.*
39 *Instrum.*, 1998, **69**, 4094-4105.
40
41 6 I. Buryakov, E. Krylov, E. Nazarov and U. Rasulev, *International Journal of Mass*
42 *Spectrometry and Ion Processes*, 1993, **128**, 143-148.
43
44 7 S. L. Isenberg, P. M. Armistead and G. L. Glish, *J. Am. Soc. Mass Spectrom.*, 2014, **25**,
45 1592-1599.
46
47 8 A. A. Shvartsburg, W. F. Danielson and R. D. Smith, *Anal. Chem.*, 2010, **82**, 2456-
48 2462.
49
50 9 E. G. Nazarov, S. L. Coy, E. V. Krylov, R. A. Miller and G. A. Eiceman, *Anal. Chem.*,
51 2006, **78**, 7697-7706.
52
53
54
55
56
57
58
59
60

- 1
2
3 10 B. Schneider, T. Covey, S. Coy, E. Krylov and E. Nazarov, *Anal. Chem.*, 2010, **82**,
4 1867-1880.
5
6
7 11 L. C. R. L. C. Rorrer and R. A. Yost, *Int. J. Mass Spectrom.*, 2011, **300**, 173-181.
8
9
10 12 U. Dharmasiri, S. L. Isenberg, G. L. Glish and P. M. Armistead, *J. Proteome Res.*,
11 2014, **13**, 4356-4362.
12
13 13 D. A. Barnett, R. Guevremont and R. W. Purves, *Appl. Spectrosc.*, 1999, **53**, 1367-
14 1374.
15
16
17 14 A. A. Shvartsburg and R. D. Smith, *J. Am. Soc. Mass Spectrom.*, 2007, **18**, 1672-
18 1681.
19
20 15 A. A. Shvartsburg, D. C. Prior, K. Q. Tang and R. D. Smith, *Anal. Chem.*, 2010, **82**,
21 7649-7655.
22
23
24 16 A. A. Shvartsburg, K. Q. Tang and R. D. Smith, *Anal. Chem.*, 2010, **82**, 32-35.
25
26
27 17 B. G. Santiago, R. A. Harris, S. L. Isenberg, M. E. Ridgeway, A. L. Pilo, D. A. Kaplan
28 and G. L. Glish, *J. Am. Soc. Mass Spectrom.*, 2015, doi: 10.1007/s13361-015-1208-9
29
30 18 A. A. Shvartsburg, K. Q. Tang and R. D. Smith, *Anal. Chem.*, 2004, **76**, 7366-7374.
31
32
33 19 A. A. Shvartsburg, F. M. Li, K. Q. Tang and R. D. Smith, *Anal. Chem.*, 2006, **78**, 3706-
34 3714.
35
36
37 20 A. Shvartsburg, Y. Ibrahim and R. Smith, *J. Am. Chem. Soc.*, 2014, **25**, 480-489.
38
39
40 21 A. A. Shvartsburg, A. J. Creese, R. D. Smith and H. J. Cooper, *Anal. Chem.*, 2011, **83**,
41 6918-6923.
42
43
44 22 A. Shvartsburg, T. Seim, W. Danielson, R. Norheim, R. Moore, G. Anderson and R.
45 Smith, *J. Am. Soc. Mass Spectrom.*, 2013, **24**, 109-114.
46
47
48 23 A. A. Shvartsburg and R. D. Smith, *Anal. Chem.*, 2011, **83**, 23-29.
49
50
51 24 J. M. Bushey, D. A. Kaplan, R. M. Danell and G. L. Glish, *Instrum. Sci. Tech.*, 2009,
52 **37**, 257-273.
53
54
55 25 E. V. Krylov, S. L. Coy, J. Vandermeij, B. B. Schneider, T. R. Covey and E. G. Nazarov,
56 *Rev. Sci. Instrum.*, 2010, **81**.
57
58
59
60